Electronic Supplementary Materials

For

Flexible low-power source-gated transistors with solution-processed metal-oxide semiconductors

Dingwei Li,[a] Momo Zhao,[b] Kun Liang,[a] Huihui Ren,[a] Quantan Wu,[c] Hong Wang[b] and Bowen Zhu*[a]*

a. Key Laboratory of 3D Micro/Nano Fabrication and Characterization of Zhejiang Province, School of Engineering, Westlake University, Hangzhou 310024, China.
E-mail: zhubowen@westlake.edu.cn

b. Key Laboratory of Wide Band Gap Semiconductor Technology, School of Microelectronics, Xidian University, Xi'an 710071, China.
E-mail: hongwang@xidian.edu.cn

c. Key Laboratory of Microelectronic Devices and Integrated Technology, Institute of Microelectronics of Chinese Academy of Sciences, Beijing 100029, China.

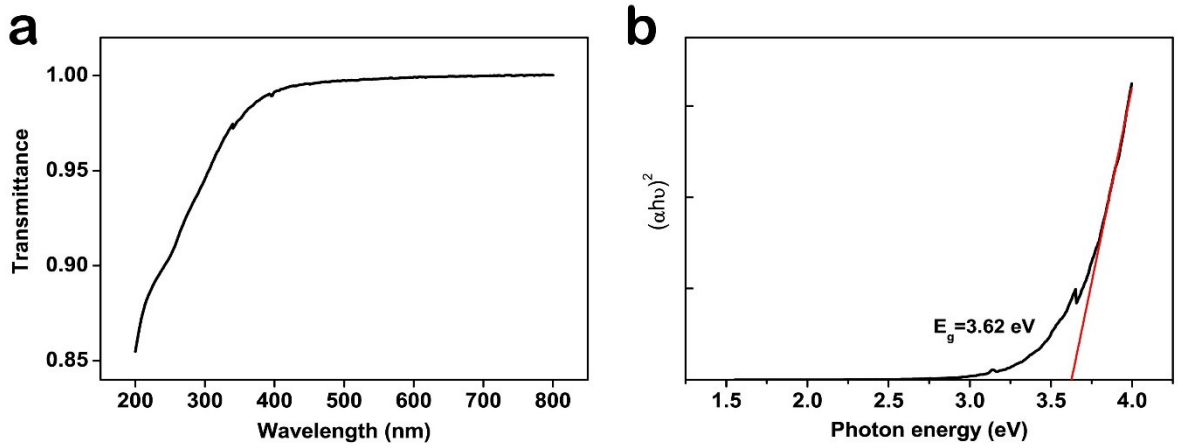

Fig. S1. UV-Vis spectrum of as prepared In_2O_3 film. (a) UV-Vis transmission spectrum of spin-coated In_2O_3 thin film on quartz substrate. (b) Tauc analysis of the absorption spectrum of In_2O_3 yields the bandgap as 3.62 eV.

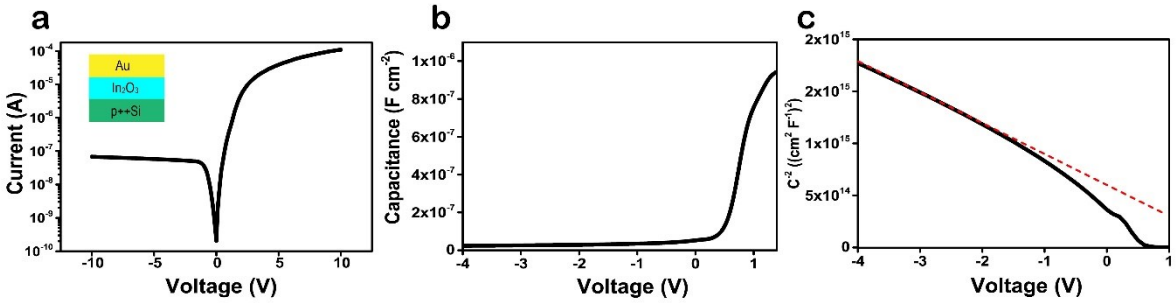

Fig. S2. Electrical and capacitance-voltage (*C-V*) measurements of $Au/In_2O_3/Si(p^{++})$ structure (inset: schamatic of structure). (a) Current-voltage (*I-V*) curve of $Au/In_2O_3/Si(p^{++})$ structure, showing a typical Schottky diode behavior with a rectification ratio ~10^3. (b) *C-V* curve of the diode. Capacitance was measured with voltage applied on Au electrode. Semiconductor capacitance (C_d) was extracted as 52.4 nF cm^{-2} at $V = 0$ V. (c) Corresponding C^{-2}-*V* plot and mean carrier concentration of In_2O_3 was extracted from the slope as 1.15×10^{17} cm^{-3}.

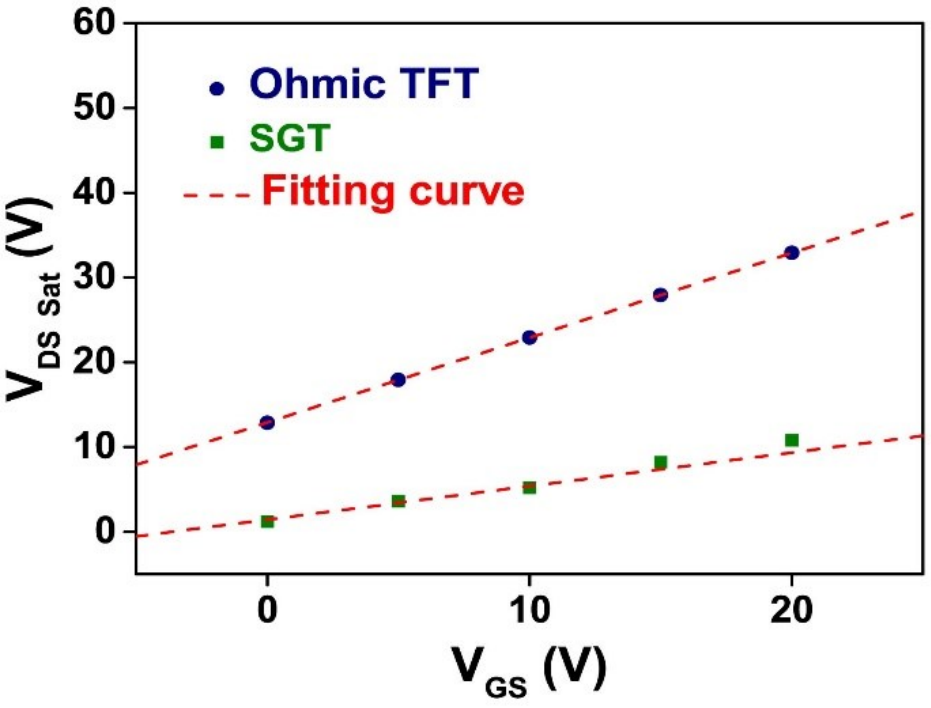

Fig. S3. Saturation voltage as a function of gate voltage for SGT and ohmic TFTs on rigid substrate with SiO_2 dielectric. SGT shows a much lower slope of ~0.2 than that of ohmic TFTs (~1).

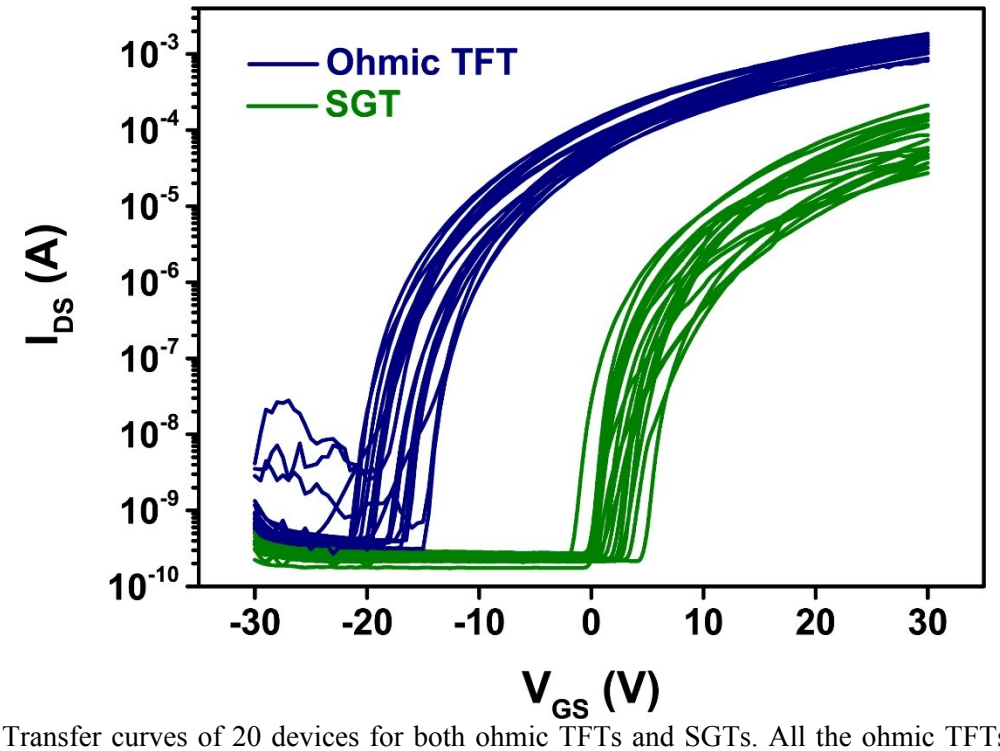

Fig. S4. Transfer curves of 20 devices for both ohmic TFTs and SGTs. All the ohmic TFTs exhibit severe negative threshold voltages (-18 ± 2.7 V). While the SGTs show positive threshold voltages (2.1 ± 1.9 V), enabling low-voltage operations.

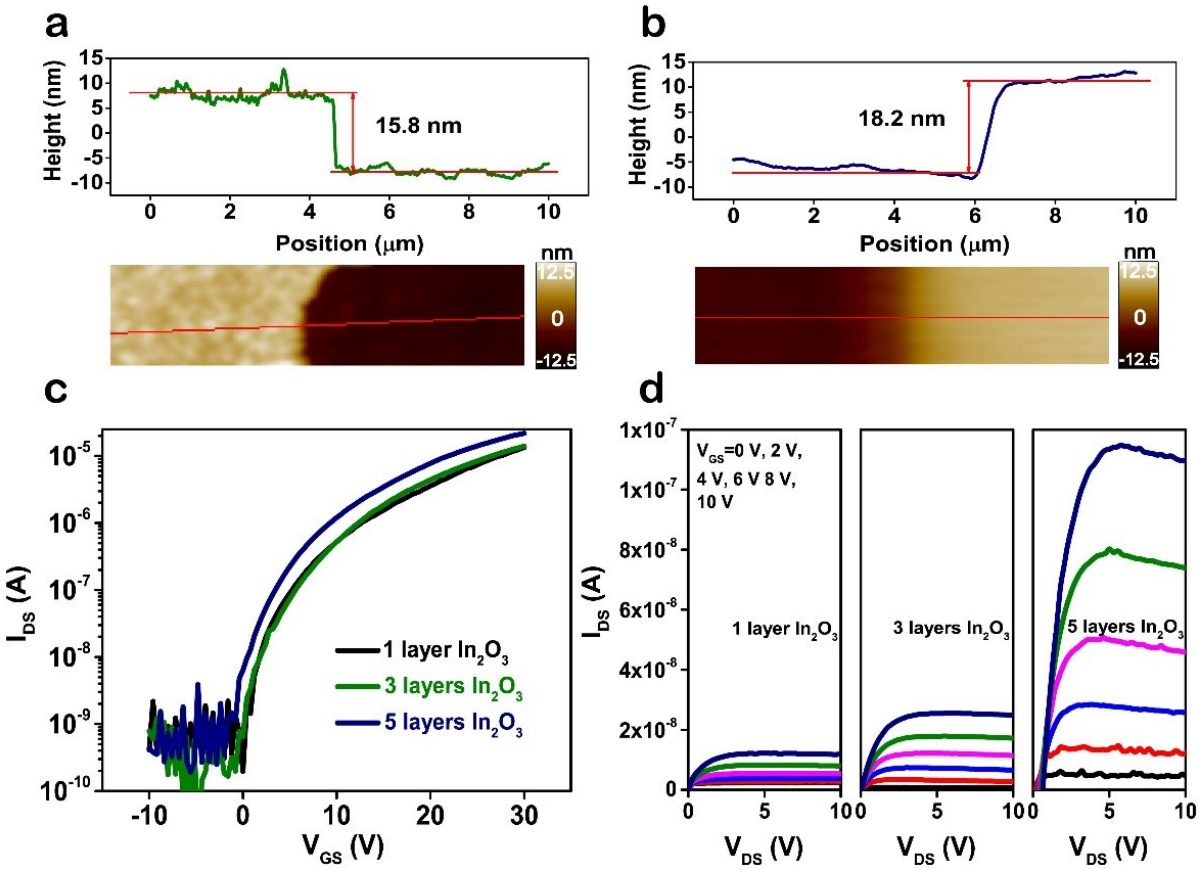

Fig. S5. Characterization of In_2O_3 SGTs with different channel thickness. (a-b) AFM height profiles (top) and corresponding AFM images (bottom) of as-prepared In_2O_3 thin films with 3 (a) and 5 (b) layers, showing thicknesses of ~15.8 and ~18.2 nm, respectively. (c-d) Transfer (c) and output (d) curves of SGTs with 1, 3, and 5 channel layers.

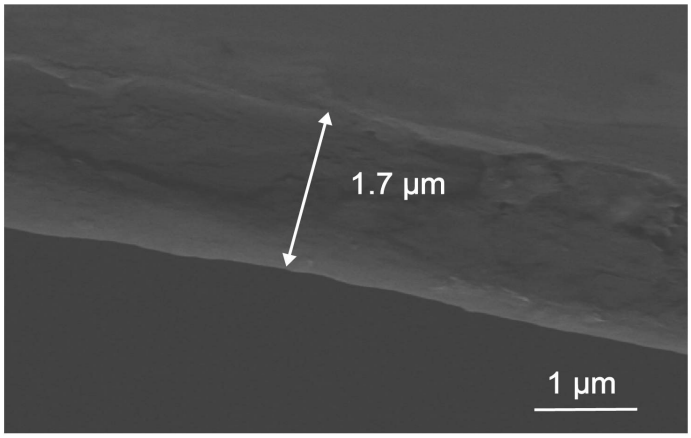

Fig. S6. Cross-sectional SEM image of spin-coated PI thin film, showing a thickness of ~1.7 µm.

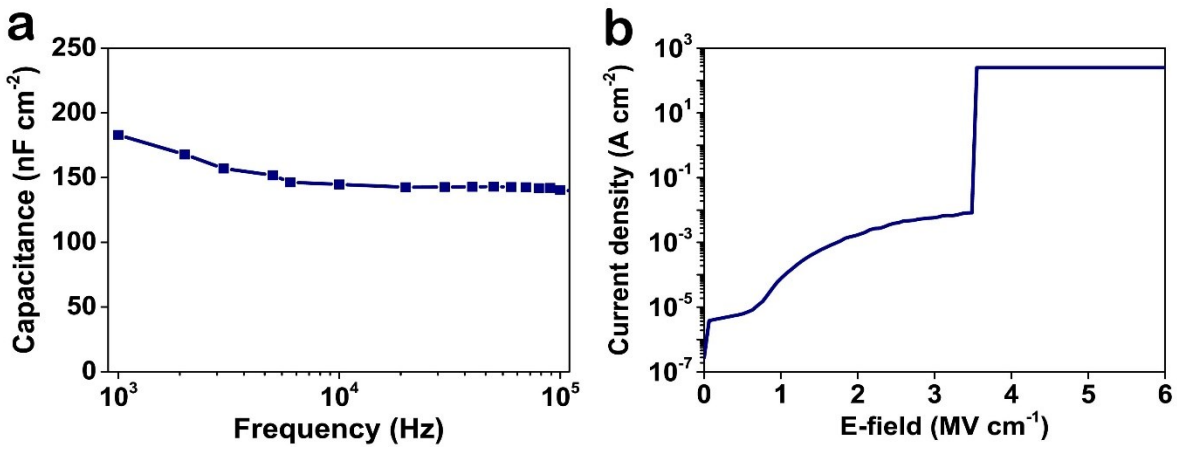

Fig. S7. Electrical performance of solution-processed Al_2O_3 dielectric layer. (a) Capacitance-frequency (*C*-*F*) and (b) Current-voltage (*I*-*V*) measurement of Au/Al_2O_3/ Si(p^{++})-based MIM capacitor. The Al_2O_3 dielectric (~30 nm thick) exhibits high capacitance of 183.0 nF cm^{-2} at 1 kHz and a high breakdown voltage of ~3.5 MV cm^{-1}.

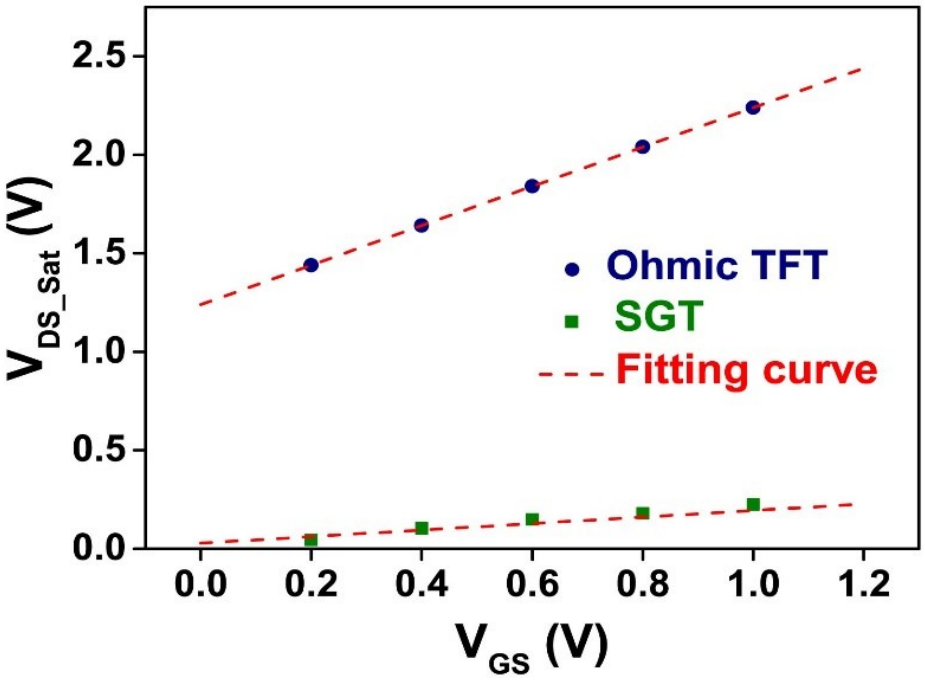

Fig. S8. Saturation voltage as a function of gate voltage for flexible SGT and ohmic TFTs on PI substrate with Al_2O_3 dielectric. SGT and ohmic TFT exhibit slopes of ~0.17 and ~1, respectively.

Table S1. Comparation of electrical and mechanical performance of TFTs with Schottky-barriers.

Channel material	Source /drain electrodes	V_{th} (V)	SS (mV dec^{-1})	Power density* (mW cm^{-2})	Intrinsic gain	Bending radius	Ref.
Polysilicon	Cr/Cr	-23	NA	400	500	NA	[1]
IGZO	Pt/Pt	3	NA	14	~29000	NA	[2]
IGZO	Mo/Mo	1.5	280	0.0075	450	NA	[3]
ZnO	Pt/Ti	-3.4	750	160	>100	NA	[4]
ZnO	Au/Al	NA	NA	50	NA	NA	[5]
C8-BTBT/PS	Ag/Ag	-0.01	60.2	0.10	~1100	NA	[6]
N2200	Au/Al	0.1	NA	10	NA	5.8 mm	[7]
In_2O_3	Au/Al	0.42	102	0.0463	~1000	5 mm	**This work**

*Power density is calculated by $P_{sat}=I_{DS\_Sat} \times V_{DS\_sat}/(W \times L)$. The saturation current (I_{DS_Sat}) and voltage (V_{DS_sat}) values are obtained from output characteristics in the references.

References:

1. R. A. Sporea, J. M. Shannon and S. R. P. Silva, *6th Conference on Ph.D. Research in Microelectronics & Electronics*, 2010, 1-4.
2. J. Zhang, J. Wilson, G. Auton, Y. Wang, M. Xu, Q. Xin and A. Song, *Proc. Natl. Acad. Sci.*, 2019, **116**, 4843.
3. S. Lee and A. Nathan, *Science*, 2016, **354**, 302.
4. A. S. Dahiya, C. Opoku, R. A. Sporea, B. Sarvankumar, G. Poulin-Vittrant, F. Cayrel, N. Camara and D. Alquier, *Sci. Rep.*, 2016, **6**, 19232.
5. A. H. Adl, A. Ma, M. Gupta, M. Benlamri, Y. Y. Tsui, D. W. Barlage and K. Shankar, *ACS Appl. Mater. Interfaces*, 2012, **4**, 1423-1428.
6. C. Jiang, H. W. Choi, X. Cheng, H. B. Ma, D. Hasko and A. Nathan, *Science*, 2019, **363**, 719-723.
7. Y. Kim, E. K. Lee and J. H. Oh, *Adv. Funct. Mater.*, 2019, **29**, 1900650.